Vacuum ultraviolet absorption and ion track effects in LiF crystals irradiated with swift ions

A. T. Davidson,[1] K. Schwartz,[2] J. D. Comins,[3] A. G. Kozakiewicz,[1] M. Toulemonde,[4] and C. Trautmann[2]
[1]*Department of Physics, University of Zululand, Kwadlangezwa 3886, South Africa*
[2]*Gesellschaft für Schwerionenforschung (GSI), Planckstr. 1, D-64291 Darmstadt, Germany*
[3]*Materials Physics Research Institute and School of Physics, University of the Witwatersrand, Johannesburg, Wits 2050, South Africa*
[4]*Centre Interdisciplinaire de Recherche Ions Lasers (CIRIL) Laboratoire CEA-CNRS-ISMRA, B.P. 5133, 14070 Caen-cedex 5, France*

(Received 16 August 2002; published 10 December 2002)

LiF crystals were irradiated with various light and heavy ions (Ni, Zn, Au, Pb, Bi, and U) of MeV to GeV energy. The radiation damage was studied by optical spectroscopy from the vacuum ultraviolet to the visible spectral region and by small angle x-ray scattering, in combination with optical bleaching and thermal annealing. In addition to the well-known electron centers (F and F_2 centers) and the hole centers responsible for the previously observed band at 114 nm, a new absorption band was observed at 121 nm. The new band appears prominently in crystals irradiated with the heaviest projectiles (Au, Pb, Bi, U), is small for Zn ions, insignificant for the lighter Ni ion and absent in case of gamma irradiation. Under optical bleaching, F- and 114-nm centers are destroyed whereas the 121-nm band is relatively stable. The decay of the 121-nm band on thermal annealing coincides with the reduction of the small-angle x-ray scattering signal. It is considered that the 121-nm band is directly linked to hole-center clusters complementary to the electron-center aggregates in the core region of ion tracks. Evidence is presented to associate an absorption band at 275 nm formed after thermal annealing with the formation of small quasi-colloidal aggregates.

DOI: 10.1103/PhysRevB.66.214102 PACS number(s): 71.55.Ht, 78.40.Ha

I. INTRODUCTION

The specific properties of damage creation in solids under swift heavy ion irradiation are a direct consequence of the high excitation density (up to several keV/nm^3) and the radial dose distribution following approximately the inverse square of the radial distance from the ion path. Owing to the strong dose gradient, defect creation and interaction processes are quite different in the region close to the ion path (track core) compared with the more extended track halo. Comprehensive studies of the track damage exist for a large number of materials[1] including radiolytic materials such as polymers[2,3] and alkali halides.[4–9] These include lithium fluoride (LiF), an ionic crystal with a large band gap energy of 14 eV that is widely used as a sensitive radiation detector or for color-center lasers.[10]

The radiation damage in LiF and in other alkali or alkaline earth halides due to classical radiation sources (gamma-rays, x rays, electrons, neutrons) has been investigated in great detail predominantly in the fifties and sixties, using various techniques such as optical absorption spectroscopy,[11–14] x-ray diffraction,[15,16] electron spin resonance,[17,18] and nuclear magnetic resonance.[19,20] In the more recent past, growing interest in the effects of ion bombardment has led to numerous investigations mainly using optical absorption.[21–28] Damage processes specifically ascribed to swift heavy ions were evidenced by additional methods including chemical etching,[6,29] small-angle x-ray scattering (SAXS),[4] swelling measurements,[8] scanning force microscopy,[30] surface sputtering,[31] and computational modeling.[32,33] Presently, the complete microstructure of the damage in ion tracks is far from being resolved. However, drawing on existing results, the following phenomenological description of different defect regions can be given:

(1) Single point defects such as F and F_2 electron centers are created in a large cylindrical halo with a radius up to 30 nm. The cross section of this halo is deduced from optical absorption studies where F and F_2 centers versus ion fluence exhibit saturation. Damage in this region is produced by the well-known excitonic mechanism which creates primary Frenkel pairs (F and H centers) and the characteristic electron and hole color centers.[9,10]

(2) An intermediate track region with a radius up to about 10 nm is ascribed to a pronounced ion-induced volume increase.[8]

(3) A much smaller track core region with a radius of 1-2 nm is deduced from SAXS experiments, which examine a cylindrical track region of modified electron density. The typical scattering pattern appears only for ions heavier than Cu.[4] There are strong indications that track etching is also directly linked to this damage in the core.[5,6]

In contrast to the creation of the well-established color centers, ion-induced swelling and chemical track etching require a critical stopping power of the ions of about 4 and 10 keV/nm, respectively.[6,8] To date, the nature of the damage in the core has not been identified, but it is reasonable to assume that defect clusters such as molecular fluorine complexes or small lithium colloids play an important role. At present, metallic colloids could not be identified by nuclear or electron spin resonance and it is not clear if such Li clusters are too small in order to exhibit metallic properties or if their density is not sufficient to be registered. Unfortunately an increase of the ion fluence for a suitable track density is problematic because severe overlapping effects of the track halo regions also lead to defect clustering, superimposing defects in the track core. Due to the fact that clusters of the electron defects in the track core are difficult to access, we decided to obtain information about the complementary hole

centers created simultaneously and in equal numbers as the electron centers.

In view of the relevance to our study, we briefly discuss current models for *V* centers, the hole center complements of electron centers (*F* centers and their aggregates). The primary halogen defect formed together with the *F* center is the *H* center being structurally equivalent to an interstitial halogen atom.[10,34] Since *H* centers become mobile at quite low temperatures, the stable configuration of interstitial halogen defects at higher temperatures are *H* center aggregates. Using near-resonance Raman spectroscopy, the characteristic vibrations of particular halogen molecular structures were detected in irradiated alkali iodides and bromides[35–43] and linked to these halogen aggregates. The dominant forms depend on the alkali halide and the temperature. The main conclusions are summarized as follows (we shall use the generic symbol *X* to stand for halogen to avoid confusion in later discussions with the use of the symbol *F* to stand for the *F* center in the case of LiF):

(i) Around 200 K in KI, RbI, and KBr,[35,41] the major defect is a di-interstitial halogen center of two *H* centers bonded to a lattice anion ($X^0X^-X^0$) or X_3^- as modeled by Catlow *et al.*[34] Higher-order halogen clusters X_n^-, $n=5,7,\ldots$ are also present. The well-known V_4 optical absorption band results collectively from the X_3^- and X_n^- defects.

(ii) For room temperature irradiation of alkali iodides and bromides with large cations Rb and Cs, the X_3^- and X_n^- defects are formed.[39,41,43] The neutral interstitial halogen molecule X_2^0 is identified in very small concentration in RbI.[41] It is noted that this latter defect was predicted to have a slightly larger binding energy than X_3^-.[34]

(iii) However, for room temperature irradiation of KI (Refs. 36,37 and 42) the dominant defects are larger halogen molecular clusters of the form $(X_2)_n$ and associated with the V_3 optical absorption band. The X_3^- and X_3^- type defects are formed in negligible concentrations. In NaBr and KBr irradiated at room temperature the three types of cluster are observed in significant concentrations.[38,39]

(iv) In KI there is a progressive development of the $(X_2)_n$ clusters and a reduction in X_3^- and X_3^- as the temperature of irradiation is raised from 200 to 300 K. The V_4 band is replaced by a steadily increasing V_3 band, these being quite close in wavelength.[40]

These studies provide a guide for LiF where similar Raman experiments on V centers have not been performed, as they would require vacuum ultraviolet excitation. It is noted that the prominent band at 114 nm in LiF (Refs. 23 and 24) was labeled V_3 based on its relative spectral position by analogy with other more widely studied alkali halides such as KBr and KCl, but without a definite knowledge of the form of halogen aggregates responsible.[44]

In the present paper, we report experiments with ion-irradiated LiF crystals using absorption spectroscopy in the vacuum ultraviolet (VUV) spectral region where processes linked to the formation and aggregation of hole centers can be studied. Since the irradiation with ions induces Frenkel defects i.e. an equal number of electron and hole centers, such investigations directly complement the existing knowledge of electronic defects obtained in the UV-vis spectral region.

In our VUV-absorption experiments, we observe a prominent new band at 121 nm which is formed efficiently in LiF bombarded with the heaviest projectiles, is insignificant for the lighter ions, and is absent for gamma ray irradiation. Complementary SAXS measurements in combination with

TABLE I. Parameters of the ion irradiation and the appearance of 121-nm absorption band. * For ions, the averaged dose D (Gy) is given by $D=1.6\times10^{-10}\ E\Phi/(\rho R)$, where E (MeV) is the total ion energy, Φ(ions/cm^2) is the fluence, $\rho=2.635$ g/cm^3 is density of LiF, and R (cm) is the range. The projectile range can be extracted by dividing the energy by the average energy loss.

Projectile	Energy (MeV)	Energy loss at surface (keV/nm)	Average energy loss (keV/nm)	Fluence (ions/cm^2)	Dose* (MGy)	121-nm band
gamma	1.2-1.3	-	-	-	0.5	absent
^{58}Ni	640	5.4	7.0	1.0×10^{11}	0.42	very small
^{68}Zn	100	10.4	7.1	6.0×10^{9}	0.03	small
				8.0×10^{10}	0.35	small
				5.0×10^{11}	2.15	small
^{197}Au	2070	24.4	23.5	4.0×10^{10}	0.57	dominant
^{208}Pb	830	28.0	21.8	1.5×10^{11}	2.0	dominant
				6.0×10^{11}	7.9	dominant
				1.2×10^{12}	15.9	
	2310	25.2	24.8	7.5×10^{10}	1.13	dominant
^{209}Bi	2040	26.3	24.9	6.8×10^{10}	1.03	dominant
				6.8×10^{11}	10.3	dominant
^{238}U	1300	31.4	24.3	5.0×10^{10}	0.74	dominant
				8.0×10^{10}	1.18	dominant
	2500	29.3	26.7	1.0×10^{10}	0.16	dominant

thermal annealing and optical bleaching allow us to ascribe this 121-nm band to the track core. A preliminary report on some of the present work was presented at a recent conference.[45]

II. EXPERIMENT

A. Irradiation

A single crystal block of high purity lithium fluoride was cleaved along the (100) plane into 0.5–1 cm^2 large platelets of thickness 0.2-0.3 mm. The crystals were irradiated with Ni, Zn, Au, Pb, Bi, and U ions of energies between 100 and 2500 MeV at the UNILAC of GSI in Darmstadt (Germany) or at the GANIL in Caen (France). All irradiations were performed at room temperature applying fluences from 6×10^9 to 1×10^{12} ions/cm^2. Under these conditions, the samples were uniformly colored in a thin surface layer corresponding to the projected ion range as calculated by the TRIM92 code.[46] Details of the irradiation parameters are presented in Table I. In addition, some selected samples were exposed to gamma rays at the Co-60 source of the Institute for Surface Modification (IOM) in Leipzig (Germany). A total gamma dose of 0.5 MGy was applied which is about three times more than for the irradiation with 2500-MeV U ions at a fluence of 10^{10} cm^{-2}.

B. Thermal annealing and optical bleaching

After irradiation, some of the samples were exposed to the light of a xenon lamp (LX175-UV from URC) or alternatively to a deuterium lamp (DUV-100W, Micropack) with a quasicontinuous spectrum in the spectral region from 200 to 500 nm. The bleaching time varied between several minutes and one hour depending on the size of the crystal and the illumination geometry. A few irradiated crystals were thermally annealed in ambient atmosphere to a temperature of 700 K. The duration of each temperature cycle was about 15 min.

III. OPTICAL ABSORPTION SPECTROSCOPY

Optical absorption (OA) spectroscopy in the ultraviolet to visible spectral region (200-700 nm) was performed with a conventional UV-vis spectrophotometer (Nicolet). In the less investigated VUV region (100–300 nm), a Rank Hilger E 760 monochromator with a sodium salicylate sensitized EMI 9558 B photomultiplier was used.

The UV-vis spectra of crystals irradiated either with ions or gamma rays typically exhibit two prominent absorption bands [Fig. 1(a)], namely, at 245 and 445 nm, assigned to F centers (halogen-ion vacancy with a trapped electron) and to F_2 centers (two F centers at nearest neighbor positions), respectively. At higher irradiation fluences when the halo of single tracks start to overlap, the spectra become more complex and additional small aggregates are present, such as F_3 centers (315 and 375 nm), F_4 centers (518 and 540 nm), and F_n^+ and F_n^- ($n\geqslant2$) centers. For a given fluence, the creation of aggregates is more pronounced in samples irradiated with heavier projectiles due to the larger halo and therefore stronger track-overlapping effects.

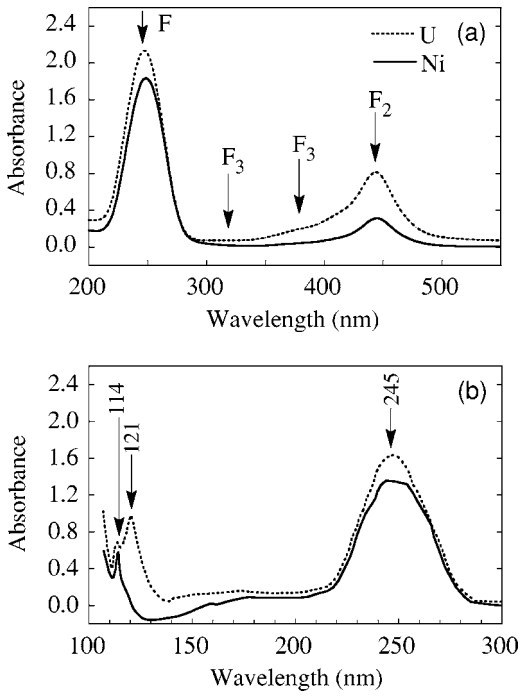

FIG. 1. Absorption spectra of LiF crystals irradiated at room temperature with 580-MeV Ni ions (solid line) of fluence 10^{11} cm^{-2} and with 1300-MeV U ions (dashed line) at a fluence of 5×10^{10} cm^{-2}. (a) In the UV-visible spectra, the two most prominent bands correspond to F and F_2 centers. (b) In the vacuum and near UV spectra, bands due to F centers (245 nm) and the complementary hole centers (114 nm) are identified. In case of irradiation with U ions, a new band appears at 121 nm.

Absorption data in the VUV region are presented in Fig. 1(b) showing as the most prominent peak the F band at 245 nm as in the UV-vis spectra. Near the band gap of the crystal, all irradiated samples exhibit a band around 114 nm with about half of the F band peak intensity. As discussed in Sec. I, this was previously labeled the V_3 band, but in view of the uncertainty of its relationship to the V_3 band in other alkali halides, and the more recent conclusions from Raman spectroscopy, we shall refer to it as the 114-nm band. Very close to the 114-nm band, an absorption band is observed with a maximum at 121 nm. This band is prominent in crystals irradiated with the heavier ions (e.g. Au, Pb, Bi or U), is very small for irradiations with lighter ion species such as Ni or Zn and is absent for irradiation with gamma rays (cf. Tab.1).

For a better understanding of the origin of the 121-nm absorption band, optical bleaching experiments were performed. In the VUV region, the effect is quite obvious for crystals irradiated with heavier ions where the new 121-nm band survives the bleaching process [Fig. 2(b)]. Note that before bleaching the maximum of the 121-nm band is too high to be measured quantitatively (optical density above 2.5). Bleaching of the Ni-ion irradiated sample causes the destruction of the prominent 245-nm band [Fig. 2(a)] and the near disappearance of the 114-nm band. However, the small

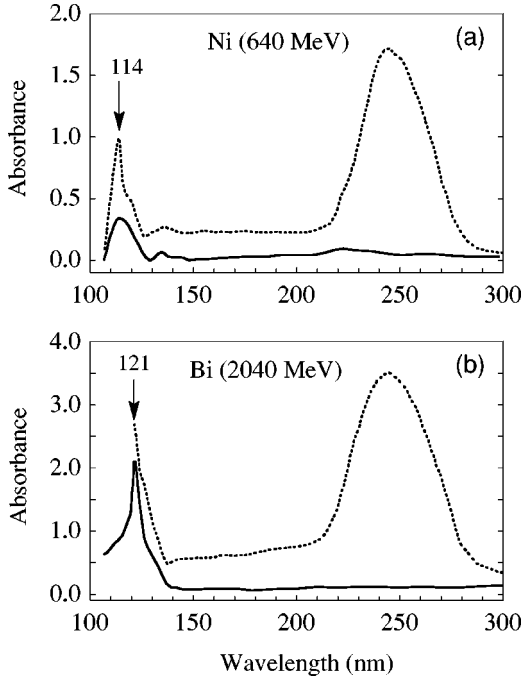

FIG. 2. Vacuum and near UV spectra of LiF crystals irradiated with (a) 640-MeV Ni ions and (b) 2040-MeV Bi ions of fluence 10^{11} cm^{-2}, before (dashed curve) and after (solid curve) optical bleaching for 10 and 14 min, respectively. The new absorption band at 121 nm survives the bleaching process.

shoulder on the 114-nm band around 121 nm remains nearly constant.

In the UV-vis region, bleaching induces a significant decrease of absorption in the entire spectral range (Fig. 3). The band of the F_2 centers disappears completely and, in the *F* center region, only some residual or background absorption persists. The residual bands are more numerous in the Bi-ion irradiated sample occurring at wavelengths of 246, 285, and 295 nm [the latter doublet has more fine structure when measured at liquid nitrogen temperature (LNT)], and at 362 nm. In the Ni-ion irradiated sample, one residual band remains at 227 nm.

We also performed isochronal thermal annealing experiments using crystals irradiated with 1300-MeV U ions of fluence 8×10^{10} cm^{-2} and 710-MeV Pb ions of fluence 10^{11} cm^{-2}. Figure 4(a) shows the annealing behavior of the *F*-, 114- and 121-nm bands for temperatures as high as 670 K. The centers responsible for the new 121-nm band are more temperature resistant than both the *F* centers and the halogen defects resulting in the 114 nm band.

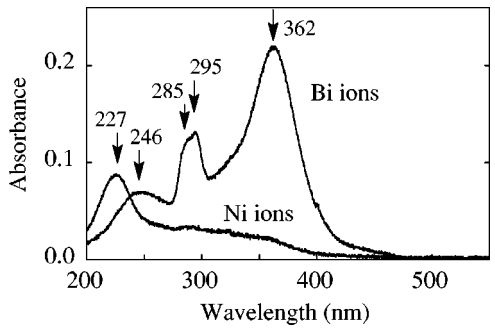

FIG. 3. Residual OA bands in the UV-vis region for LiF crystals irradiated with 640-MeV Ni ions (10^{11} cm^{-2}) and with 2040-MeV Bi ions (6.8×10^{10} cm^{-2}), bleached with UV light for about 10 and 20 min, respectively.

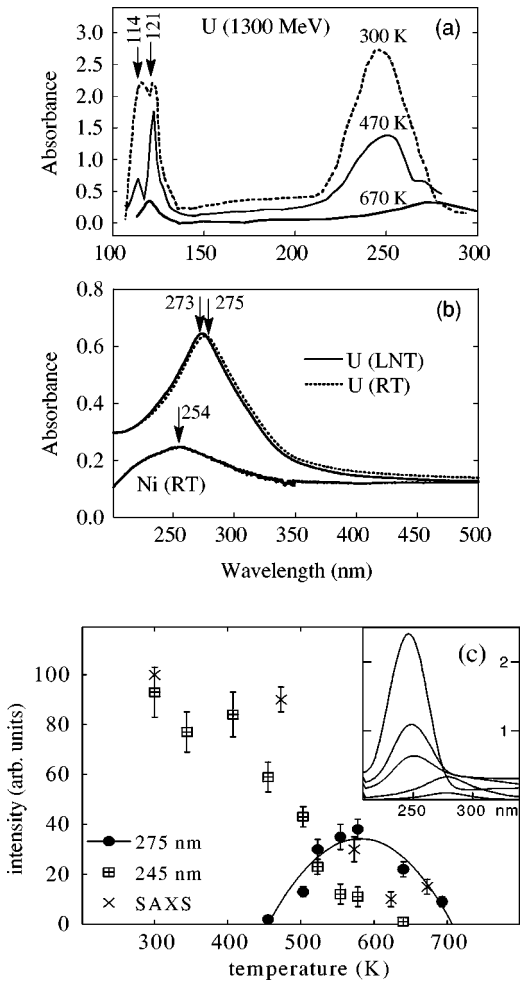

FIG. 4. (a) Vacuum and near UV spectra of a LiF crystal irradiated with 1300-MeV U ions (8×10^{10} cm^{-2}) at room temperature (dashed curve) and after annealing at 470 and 670 K (solid curves). (b) UV-vis absorption spectra after isochronal annealing at 680 K. The spectra were measured at room temperature (RT) and at liquid nitrogen temperature (LNT). The irradiations were performed with 1300-MeV U ions (8×10^{10} cm^{-2}) and with 640-MeV Ni ions (10^{11} cm^{-2}). (c) Intensity of F centers (245 nm), 275-nm band, and normalized SAXS signal as a function of annealing temperature for samples irradiated with 710-MeV Pb ions (10^{11} cm^{-2}). The inset shows the corresponding absorption spectra for annealing temperatures at various stages (358, 508, 558, 693, and 774 K). The decrease of the *F* centers correlates with the appearance of the 275-nm band.

The UV-vis absorption spectrum of the same crystals exhibits a broad residual band produced at 275 nm [Fig. 4(b)]. Its half-width and peak position are unaffected when the spectrum is measured at LNT, a typical behavior for metallic colloids. A detailed study of the evolution of this 275-nm

band as a function of temperature was performed for samples irradiated with Pb ions [Fig. 4(c)]. The decay of the *F*-center band and the growth of the 275-nm band are correlated, whereas the final annealing of the latter band (275 nm) occurs in the same range of temperatures as the SAXS signal. In the case of irradiation with the lighter ions (640-MeV Ni, 10^{11} ions/cm^2), the annealed sample did not produce the band at 275 nm, at the relatively low fluence used here. However, it was observed when annealing high fluence samples irradiated with S ions (10^{13} ions/cm^2) or Zn ions (5×10^{11} ions/cm^2).

IV. SMALL-ANGLE X-RAY SCATTERING

As described earlier, ion-irradiated LiF can be studied by small-angle x-ray scattering where the highly anisotropic scattering pattern indicates the creation of the core region of tracks.[5,7] When analyzing the scattered intensity, the shape of the track is assumed to have cylindrical geometry with the z-axis corresponding to the ion trajectory. In addition, we suppose that the radial density variation follows a Gaussian distribution. The scattered x-ray intensity in the reciprocal space $I(k_r,k_z)$ is then given by

$$I(k_r,k_z)=N\Delta\rho^2\times4\pi^2\times r^4\times\sin^2(k_z\times L/2)/k_z^2 \times\exp(-k_r^2\times r^2/2),$$

where L is the length of the track which corresponds approximately to the range of the ions, N is the number of tracks, and k_r and, k_z are the momentum vectors respectively perpendicular and parallel to the ion path. The perpendicular component is $k_r=4\pi/(\lambda\sin\Theta)$, where $\lambda=1.54$ Å is the wavelength of the x-ray beam and 2Θ denotes the scattering angle. The parameter $\Delta\rho$ is the maximum electron density difference between the tracks and the undamaged surrounding material. The value r gives a mean track radius defined by the Gaussian radius at which $\Delta\rho$ decreases to e^{-1}. Using a Guinier plot ($\ln I\sim k_r^2$), the track radius can be determined from the slope of a straight line fitted to the intensity data.[47] The SAXS data of LiF crystals irradiated with 1300-MeV U ions at a fluence of 8×10^{10} ions/cm^2 are presented in Fig. 5. The radius analysis gives for the track core a value of 1.6 nm, in good agreement with earlier results.[4,5,7]

The same crystals were also exposed to optical bleaching and thermal annealing over the range 300–670 K. After 50 min of bleaching, the *F* band completely disappeared, but most notably, the SAXS pattern did not exhibit any modification either concerning the intensity or the deduced track radius. Under thermal annealing for 15 min at 670 K, the intensity of the scattering pattern becomes much weaker indicating a decrease of $\Delta\rho^2$, while the extracted radius does not alter, as demonstrated by the unchanged slope of the two data sets in Fig. 5. For a quantitative evaluation of this intensity decrease, the $\Delta\rho^2(T)$ data were deduced for samples annealed at different temperatures ($\Delta\rho^2(T)\sim I(T)r^{-4}(T)\exp[r^2(T)k_r/2]$) and then normalized to $\Delta\rho^2$(300 K) of a room temperature sample. Figure 6 presents the $\Delta\rho^2(T)/\Delta\rho^2$(300 K) data as a function of the annealing temperature. A comparison of the temperature evolution of the SAXS data and the absorbance of the 121-nm band shows a clear correlation (Fig. 6).

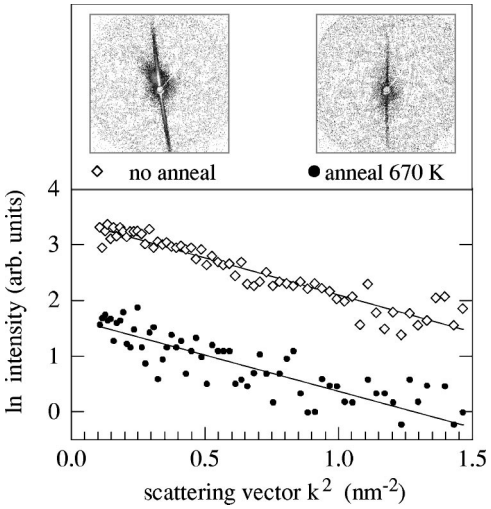

FIG. 5. SAXS data of a LiF crystal irradiated with 1300-MeV U ions at a fluence of 8×10^{10} cm^{-2}. Top: anisotropic distribution of scattered x-ray intensity on (10×10 cm^2) area detector. Bottom: scattered x-ray intensity vs the square of the scattering vector before (open diamonds) and after annealing at 670 K (filled circles).

V. DISCUSSION

Irradiation of LiF crystals with swift light and heavy ions leads to the creation of primary Frenkel defects (*F*-*H* pairs) which eventually form various defect structures in the core and halo regions of the ion tracks. Since electron and hole centers appear in pairs, the cylindrical region around each ion trajectory should contain electron centers (*F* centers, F_n centers, colloids, etc.) and hole centers (fluorine molecular centers and their aggregates) in stochiometric equilibrium. From optical absorption studies of coloration versus ion fluence, it is known that simple *F* and F_2 centers are located mainly in the halo region which extends several tens of nm. There have been few investigations of the complementary halogen defects responsible for the 114-nm band because the

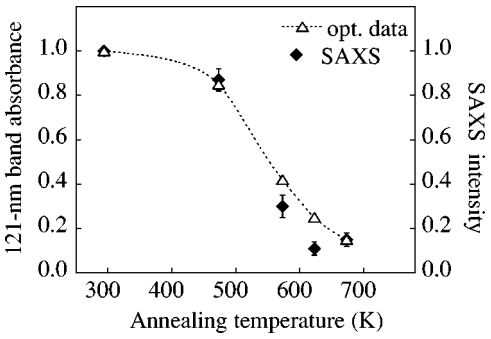

FIG. 6. Evolution of normalized SAXS data [$\Delta\rho^2(T)/\Delta\rho^2$(300 K)] and 121-nm band absorbance as a function of annealing temperature (the dotted line is drawn to guide the eye). The LiF crystals were irradiated with 1300-MeV U ions at a fluence of 8×10^{10} cm^{-2}.

experimental access via VUV spectroscopy is more complicated.

Optical bleaching using light within the F band leads to the excitation of F centers to become F^* centers. Owing to a decrease of the activation energy in the excited state, F^* centers exhibit an enhanced thermal diffusion. Their high mobility has a strong effect on secondary reactions such as recombination with V centers or aggregation.[33,48] Bleaching induced the disappearance of the F band at 245 nm together with the drastic drop in intensity of the 114-nm band indicating that the respective centers are strongly involved in the recombination process occurring in the track halo. The bleaching results strongly support interstitial halogen defects as being responsible for the 114-nm band.

As discussed in Sec. I, the detailed microstructure of the defects responsible for the 114-nm band in LiF has not yet been determined with any degree of certainty. Raman spectroscopy performed on other alkali halides indicates several possible structures for the responsible fluorine aggregates. However, earlier experiments on KBr and KCl,[49–53] now further interpreted in the light of the more recent Raman studies, have shown that the X_3^- defects responsible for the V_4 band have lower thermal stability. Moreover, these X_3^- defects are readily reduced during F-band bleaching as compared with the interstitial cluster defects of the type $(X_2)_n$ responsible for the V_3 band that are resistant to F-band bleaching. Thus the mutual reduction of the F band and the 114-nm band during such bleaching suggests that the latter is more likely due to a smaller cluster type such as X_3^-.

On the supposition that optical bleaching eliminates the better understood color centers formed in the halo, the residual spectra must arise from different electron- and hole-center aggregates unaffected by bleaching. In strong contrast to the 114-nm centers and the F centers in the halo, the 121-nm band is not destroyed under bleaching, indicating a correlation with the track core. This assumption is corroborated by the finding that the 121-nm band appears primarily in crystals irradiated with the heavier ions and is small or insignificant in samples irradiated with the lighter ions and gamma rays. Moreover, the optical bleaching and thermal annealing behavior of the 121-nm band shows a good agreement with the SAXS signal that is directly ascribed to the core damage. It is noted that chemical track etching for projectiles above a critical stopping power of about 10 keV/nm is observed. Table I indicates that for Zn this is achieved at the surface and the small but measurable 121-nm band is consistent with this result.

To date, the details of the microstructure of the damage in the track core have not been identified. With regard to the electron centers, the UV-vis spectra are dominated by the strong absorption of F and F_2 centers and at larger fluences the higher order F_3 and F_4 centers; therefore the additional optical absorption of the electron-center aggregates from the core is not easily accessible. There are some differences between bleached samples irradiated with light Ni ions or heavy Bi ions. The residual spectra exhibit a weak absorption band at 227 nm for Ni and some absorption bands at 285–295 nm and at 360 nm for Bi. These bands produced during bleaching are probably due to specific F-center aggregates.[11,54] Additional experiments and a detailed analysis of residual bleaching spectra may help to identify such defects.

Thermal annealing also leads to some interesting observations, namely, the appearance of a band near 275 nm showing the properties of metallic colloids[54] or F-center aggregates.[55] Due to limited data, it is not immediately clear if this band results from the halo or from the core of the tracks. Based on the observation that the band was not observed with Ni-ion bombardment and only at high fluences with Zn and S ions, we consider it a reasonable supposition that the band is associated with the core of the tracks. Finally it should be mentioned that the 275-nm band has been reported on several occasions in the literature.[54,56,57] In an investigation by Politov and Vorozheikina of neutron irradiated LiF,[57] the defects responsible were discussed in terms of the finest colloidal particles of lithium, a quasicolloidal precursor consisting of clustered F centers. It is noted that these quasicolloidal centers do not yield an electron spin resonance signal. Also relevant are the recent computer simulations[33] carried out to investigate the formation of F_n or nF aggregates in ion tracks during heavy ion bombardment of LiF. For realistic values, the F-center aggregation process leads to extremely small clusters in the core region containing a few F centers or Li atoms. These model calculations appear to have features in common with the quasicolloidal centers discussed in Ref. 56. In support, LiF crystals irradiated with heavy ions did not show any electron spin resonance signal from metallic Li colloids. These arguments lend support to the concept that the 275-nm band is associated with the track core. However, at sufficiently high fluences with sub or near threshold ions (S and Zn) where clear track overlap effects occur, the 275-nm band could also be produced by annealing. Thus additional high fluence experiments with Ni ions are necessary to confirm the location (core or halo) of the defects responsible for the 275-nm band. Based on these arguments, it is likely that the formation of the 275-nm band is the consequence of the presence of small aggregates F_n predicted computationally to be formed within the track cores.

The defects responsible for the 121-nm band reported here are the first that are clearly related to the track core. The interstitial fluorine clusters responsible are thus different from those resulting in the 114-nm band and located in the halo region. In particular, they have a higher thermal stability and a substantial resistance to optical bleaching within the F band. As already discussed, we favor the X_3^- aggregate as the defect responsible for the 114-nm band. In view of the restricted geometry of the ion tracks and by analogy with the small F center aggregates F_n, a possible structure for the 121-nm defects would be a small or embryo form of the molecular $(X_2)_2$ clusters. These, when formed, have the required higher thermal stability and the resistance to F band bleaching as compared with the X_3^- aggregates. In this context, it should be emphasized that the formation of gaseous halogen molecules as discussed for various irradiated alkali halides is unlikely mainly because defects clusters created by, e.g., thermal neutrons are much larger compared to defects induced by swift heavy ions at the present fluences. In addition, the expected absorption spectrum from fluorine

F_2-gas molecules is quite different from the observed 121-nm band.[58–61]

VI. CONCLUSIONS

LiF crystals were irradiated with various heavy ions of MeV-GeV energy. Using VUV absorption spectroscopy, an absorption band was discovered at 121 nm, located close to the previously investigated 114-nm band. The new band has the following characteristics: (1) It appears primarily for crystals irradiated with projectiles heavier than Zn ions. This threshold is in good agreement with SAXS data and with the critical energy loss for chemical track etching around 10 keV/nm. (2) It survives bleaching when bands ascribed to simple color centers such as *F* centers (245 nm) and the *V* centers responsible for the 114-nm band disappear. (3) Its temperature dependence on annealing exactly mimics the SAXS signal, the band being more stable at higher temperatures than color centers produced by classical radiation sources. The evidence suggests that the new band at 121 nm is attributable to clusters of fluorine interstitial hole centers complementary to the electron- center aggregates, the latter being located in the core region of the ion tracks. Possible structures are suggested for both the 121-nm band and the 114-nm band. Studies of a band near 275 nm produced by annealing irradiated crystals are reported. It is considered that quasicolloidal centers are responsible but their precise location requires further investigations.

ACKNOWLEDGMENTS

We thank Dr. W. Knolle for the gamma irradiations at the IOM and D. J. Wilkinson and G. Christopulo for technical assistance at the VUV spectrometer. At UZ, the work was supported by the Research Committee of Zululand University and by the National Research Foundation of South Africa (NRF). J.D.C. received support from the University of the Witwatersrand Research Committee, the Faculty of Science and the NRF. K.S., M.T., and C.T. acknowledge the support given by the European Commission under EC-HPRI-CT-1999-00001.

[1] See, e.g., *Proceedings of the Fourth International Conference on Swift Heavy Ions in Matter (SHIM 98), Berlin, 1998*, edited by S. Klaumünzer and N. Stolterfoht [Nucl. Instrum Methods Phys. Res. B **146** (1998), Sec. III, p.206].
[2] E. Balanzat, S. Bouffard, A. LeMoël, and N. Betz, Nucl. Instrum. Methods Phys. Res. B **91**, 140 (1994).
[3] T. Steckenreiter, E. Balanzat, H. Fuess, and C. Trautmann, Nucl. Instrum. Methods Phys. Res. B **151**, 161 (1999).
[4] K. Schwartz, C. Trautmann, T. Steckenreiter, O. Geiss, and M. Kramer, Phys. Rev. B **58**, 11232 (1998).
[5] K. Schwartz, G. Wirth, C. Trautmann, and T. Steckenreiter, Phys. Rev. B **56**, 10711 (1997).
[6] C. Trautmann, K. Schwartz, and O. Geiss, J. Appl. Phys. **83**, 3560 (1998).
[7] K. Schwartz, A. Benyagoub, M. Toulemonde, and C. Trautmann, Radiat. Eff. Defects Solids **155**, 127 (2001).
[8] C. Trautmann, M. Toulemonde, J.M. Costantini, J.J. Grob, and K. Schwartz, Phys. Rev. B **62**, 13 (2000).
[9] C. Trautmann, M. Toulemonde, K. Schwartz, J.M. Costantini, and A. Müller, Nucl. Instrum. Methods Phys. Res. B **164-165**, 365 (2000).
[10] N. Itoh and A.M. Stoneham, in *Materials Modification by Electronic Excitation* (Cambridge University Press, Cambridge, 2001).
[11] C.J. Delbecq and P. Pringsheim, J. Chem. Phys. **21**, 794 (1953).
[12] S. Mascarenhas, D.A. Wiegand, and R. Smoluchowski, Phys. Rev. **134**, A485 (1964).
[13] J.D. Comins and P.T. Wedepohl, J. Phys. C **1**, 906 (1968).
[14] M.R. Mayhugh, J. Appl. Phys. **41**, 4776 (1970).
[15] H. Peisl, W. Kampfhammer, and W. Waidelich, Solid State Commun. **2**, 167 (1964).
[16] M. Lambert, Ch. Mazieres, and A. Guinier, J. Phys. Chem. Solids **18**, 129 (1961).
[17] W. Känzig and T.O. Woodruff, J. Phys. Chem. Solids **9**, 70 (1958).
[18] R. Kaplan and P.J. Bray, Phys. Rev. **129**, 1919 (1963).
[19] C.D. Knutsen, H.O. Hooper, and P.J. Bray, J. Phys. Chem. Solids **27**, 147 (1966).
[20] P.J. Ring, J.G. O'Keefe, and P.J. Bray, Phys. Rev. Lett. **1**, 453 (1958).
[21] P. Thévenard, G. Guirand, C.H.S. Dupuy, and B. Delaunay, Radiat. Eff. Defects Solids **32**, 83 (1977).
[22] A. Perez, J. Davenas, and C.H.S. Depuy, Nucl. Instrum. Methods **132**, 219 (1972).
[23] A.T. Davidson, J.D. Comins, and T.E. Derry, Radiat. Eff. **90**, 213 (1985).
[24] A.T. Davidson, J.D. Comins, T.E. Derry, and F.S. Khumalo, Radiat. Eff. **98**, 305 (1986).
[25] L.H. Abu-Hassan and P.D. Townsend, J. Phys. C **19**, 99 (1986).
[26] A. Perez, E. Balanzat, and J. Dural, Phys. Rev. B **41**, 3943 (1990).
[27] J.D. Comins, A.T. Davidson, and T.E. Derry, Defect Diffus. Forum **57-58**, 409 (1988).
[28] P.D. Townsend, Rep. Prog. Phys. **50**, 501 (1987).
[29] R.L. Fleischer, P.B. Price, and R.M. Walker, J. Appl. Phys. **36**, 3645 (1965).
[30] A. Müller, R. Neumann, K. Schwartz, T. Steckenreiter, and C. Trautmann, Nucl. Instrum. Methods Phys. Res. B **146**, 393 (1998).
[31] M. Toulemonde, W. Assmann, C. Trautmann, and F. Grüner, Phys. Rev. Lett. **88**, 057602 (2002).
[32] M. Toulemonde, Ch. Dufour, A. Meftah, and E. Paumier, Nucl. Instrum. Methods Phys. Res. B **166-167**, 903 (2000).
[33] E.A. Kotomin, V. Kashcheyevs, V.N. Kuzovkov, K. Schwartz, and C. Trautmann, Phys. Rev. B **64**, 144108 (2001).
[34] C.R.A. Catlow, K.M. Diller, and L.W. Hobbs, Philos. Mag. A **42**, 123 (1980).
[35] L. Taurel, E. Rzepka, and S. Lefrant, Radiat. Eff. **12**, 115 (1983).
[36] E. Rzepka, S. Lefrant, L. Taurel, and A.E. Hughes, J. Phys. C **14**, L767 (1981).

[37] A.M.T. Allen and J.D. Comins, Cryst. Lattice Defects Amorphous Mater. **17**, 93 (1987).
[38] E. Rzepka, M. Bernard, S. Lefrant, and J.D. Comins, Cryst. Lattice Defects Amorphous Mater. **17**, 113 (1987).
[39] M. Bernard, E. Rzepka, and S. Lefrant, Radiat. Eff. Defects Solids **116**, 259 (1991).
[40] A.M.T. Allen and J.D. Comins, Nucl. Instrum. Methods Phys. Res. B **65**, 516 (1992).
[41] A.M.T. Allen and J.D. Comins, J. Phys.: Condens. Matter **4**, 2701 (1992).
[42] J.D. Comins, A.M.T. Allen, E. Rzepka, and S. Lefrant, Radiat. Eff. Defects Solids **136**, 295 (1995).
[43] M.A. Pariselle, S. Lefrant, E. Balanzat, B. Ramstein, and J.D. Comins, Phys. Rev. B **53**, 11365 (1996).
[44] M.R. Mayhugh and R.W. Christy, Phys. Rev. B **2**, 3330 (1976).
[45] A.T. Davidson, J.D. Comins, A.G. Kozakiewicz, K. Schwartz, and C. Trautmann, Nucl. Instrum. Methods Phys. Res. B **191**, 212 (2002).
[46] J.F. Ziegler, J.P. Biersack, and U. Littmark, in *The Stopping and Ranges of Ions in Matter*, edited by J.F. Ziegler (Pergamon, New York, 1985).
[47] D. Albrecht, P. Armbruster, R. Spohr, M. Roth, K. Schaupert, and H. Stuhrmann, Appl. Phys. A: Solids Surf. **A37**, 37 (1985).
[48] A. Rascón and J.L. Alvarez Rivas, J. Phys. C **16**, 241 (1983).
[49] W.A. Sibley and E. Sonder, Phys. Rev. Lett. **14**, 900 (1965).
[50] J.D. Comins and P.T. Wedepohl, Solid State Commun. **4**, 537 (1966).
[51] E. Sonder, W.A. Sibley, J.E. Rowe, and C.M. Nelson, Phys. Rev. **153**, 1000 (1967).
[52] J.D. Comins, Solid State Commun. **5**, 709 (1967).
[53] J.D. Comins, Phys. Status Solidi B **43**, 101 (1971); **43**, 113 (1971).
[54] A.E. Hughes and S.C. Jain, Adv. Phys. **28**, 717 (1979).
[55] A.B. Scott and W.A. Smith, Phys. Rev. **83**, 982 (1951).
[56] K.K. Schwartz, A.A. Vitol, A.V. Podin, D.O Kalnin, and Yu.A. Ekmanis, Phys. Status Solidi **15**, 897 (1966).
[57] N.G. Politov and L.F. Vorozheikina, Fiz. Tverd. Tela (Leningrad) **12**, 343 (1970) [Sov. Phys. Solid State **12**, 277 (1970)].
[58] L.W. Hobbs, J. Phys. (Paris), Colloq. **37**, C-7 (1976).
[59] E.A. Colbourn, M. Dagenais, A.E. Douglas, and J.W. Raymonda, Can. J. Phys. **54**, 1343 (1976).
[60] *Gmelin Handbuch der Anorganischen Chemie, Fluorine, Suppl.* (Springer Verlag, Berlin, 1980), Vol. 2, pp. 53–59.
[61] A.B. Lidiard, Comments Solid State Phys. **8**, 73 (1978).